



Preparation of a novel and highly stable Al-Fe loaded sepiolite catalyst for the CWPO of methyl orange: Optimization of physicochemical parameters, kinetics and thermodynamics studies

İlker Kıpçak* & Esin Kalpazan

Department of Chemical Engineering, Eskişehir Osmangazi University, Eskişehir, Turkey
E-mail: ikipcak@ogu.edu.tr

Received 7 December 2019; accepted 2 September 2020

Al-Fe loaded sepiolite catalysts with different active metal ratio have been synthesized using a Turkish sepiolite sample from Eskişehir region. Liquid phase catalytic oxidation of methyl orange azo dye has been carried out over Al-Fe/sepiolite catalysts using hydrogen peroxide as oxidant. The catalytic studies are performed in a glass reactor under atmospheric pressure by semi-batch operation. The effects of several parameters such as catalyst amount, metal loading, calcination temperature, pH, H₂O₂ concentration, reaction temperature and time on the methyl orange elimination have been examined. The elimination rate of 90.68% was achieved when studied with the catalyst with 8% active metal ratio (SepAlFe8) at pH 3.7 and 25°C. Kinetics studies show the degradation of methyl orange over the SepAlFe8 catalyst could be expressed by the pseudo-first-order reaction kinetics ($k_1 = 0.0049 \text{ min}^{-1}$ at 25°C). The activation energy (E_a) of the reaction over this catalyst is found as 29.48 kJ mol⁻¹. It was also found that the catalytic oxidation process is endothermic ($\Delta H = 26.99 \text{ kJ mol}^{-1}$) and nonspontaneous ($\Delta G = 96.72 \text{ kJ mol}^{-1}$ at 25°C). The catalyst is chemically stable and reusable with low release of iron.

Keywords: Catalyst characterization, Catalytic wet peroxide oxidation (CWPO), Kinetics, Methyl orange, Sepiolite, Thermodynamics

The pollution of water resources by large quantities of dye effluents generated from several industries such as paint, textile, paper, plastics, food and cosmetics has a negative environmental impact, affecting the quality of drinking water for the next generation¹. The fact that dyes are used for specific applications requiring their resistance to the environmental conditions leads to dye effluents having intensive color, high chemical and optical steadiness and non-biodegradable properties². Some physicochemical techniques are available for the treatment of the dye effluents. However, the application of physical methods such as adsorption, flocculation and reverse osmosis has the inherent disadvantages of being non-destructive, since they only transfer dye from wastewater effluent, thus causing secondary contamination. Chemical methods such as chlorination and ozonation are also used to remove certain dyes, but they are not economically feasible and involve complex procedures³. In this context, advanced oxidation processes (AOPs) are an attractive alternative for the degradation of dyes and for the destruction of a wide range of other organic compounds⁴. Among the AOP, catalytic wet peroxide oxidation (CWPO) is recognized as a low-cost technology since it relies on

very simple technology and operates under mild conditions (20-80°C and atmospheric pressure). CWPO uses a suitable catalyst to promote the partial decomposition of hydrogen peroxide (H₂O₂) to hydroxyl radicals ($\bullet\text{OH}$) which are highly oxidizing species and can efficiently degrade most of the organic pollutants in wastewater. Moreover, H₂O₂ is an environmentally friendly agent because the decomposition products are only oxygen and water. This makes CWPO based water treatment technologies more environmentally attractive⁵. The major drawback of using CWPO process is its dependence on a metal (Fe, Cu etc.) based heterogeneous catalyst that requires certain operating conditions (such as low pH and high temperature) to achieve satisfactory catalytic activity. In addition, there is always a concern about the stability of the catalyst during the CWPO operation². Selecting a proper synthesis method and an appropriate support material, and also optimizing the operating conditions may enhance the catalytic activity and stability of the catalyst. Clay minerals, zeolites, silica, alumina and activated carbon are some of frequently used support materials in the CWPO processes⁶.

Sepiolite is a natural hydrated magnesium phyllosilicate with fibrous morphology due to its crystalline structure. The unit cell formula of the mineral is $\text{Mg}_8\text{Si}_{12}\text{O}_{30}(\text{OH})_4(\text{H}_2\text{O})_4 \cdot 8\text{H}_2\text{O}$ ⁷. Structurally, it is formed by an alteration of blocks and channels growing up in the fibre direction. Each block is constructed of two tetrahedral silica sheets and a central octahedral magnesia sheet. Due to the discontinuity of the external silica sheet, a significant number of silanol (Si-OH) groups are present at the surface of the mineral⁸. Sepiolite has a high specific surface area (80-350 $\text{m}^2 \text{g}^{-1}$) by means of its small sized particles, fibrous morphology and intracrystalline tunnels⁹. In addition, the unique fibrous structure with interior channels allows the penetration of organic and inorganic ions into the structure of sepiolite and makes it a valuable material for a wide range of industrial applications¹⁰. In the last years, this mineral has become one of the most important and useful industrial minerals¹¹. Sepiolite is commonly used as catalyst, catalyst support, filler, membrane, molecular sieve and adsorbent¹⁰. Several deposits of sepiolite have been reported in Turkey. The most commercially-important sepiolite deposits are located in the Eskişehir province (west central Anatolia). Türkmentokat-Gökçeoğlu region is the most important and high quality sepiolite mining district in Eskişehir. These sepiolite from this region is mostly used to make tobacco pipes (known as meerschaum pipes) and decorative objects by carving because of its unique properties such as adsorption, chemical composition, white color, good porosity and low specific gravity. It was reported that the adsorption capacity of "right" meerschaum was better than that of activated carbon¹².

To our knowledge, no study has explored the performance of Al-Fe loaded sepiolite in azo dye degradation although the several catalytic applications of sepiolite based composites were examined by some researchers¹³⁻¹⁶. In the present study, it was aimed to prepare a highly stable and effective Al-Fe loaded sepiolite catalyst for using in the CWPO of methyl orange azo dye. The natural sepiolite and the catalysts were characterized by XRD, XRF, BET, SEM and EDX analyses. The effects of catalyst amount, metal loading, calcination temperature, pH, H_2O_2 concentration, reaction temperature and time on the elimination of the dye were explored. The catalytic process was also studied from kinetics and thermodynamics perspectives.

Experimental Section

Materials

The natural sepiolite (Sep) used in this study was supplied from a workshop as carving residue of a nodular type sepiolite (meerschaum) which was excavated from Türkmentokat-Gökçeoğlu district in Eskişehir. The clay sample was ground, sieved through a 200 mesh ASTM standard sieve and then dried at 105°C for 3 hours. All chemicals used in the experimental studies were purchased as of analytical purity and all solutions were prepared with distilled water. A stock solution containing 1000 mg L^{-1} of methyl orange (MO) was prepared by dissolving a predetermined amount of the dye in distilled water. The stock was diluted with distilled water to prepare desired working solutions.

Preparation of catalysts

A sepiolite sample of 2 g was weighed and put in a glass beaker and 0.1 L of distilled water was slowly poured on it to compose a clay-water suspension of 2 wt. %. The suspension was stirred with a magnetic stirrer at the rate of 400 rpm for 24 hours at room temperature. In another beaker, a solution with total volume of 50 mL was prepared by mixing various volumes of 0.2 M $\text{Al}(\text{NO}_3)_3 \cdot 9\text{H}_2\text{O}$ and 0.2 M $\text{Fe}(\text{NO}_3)_3 \cdot 9\text{H}_2\text{O}$ to reach the desired active metal ratio (AMR) changing from 0 to 10%. Thereafter, to get the hydrolysis ratio (OH/Fe+Al) of 2.0, a 100 mL of 0.2 M NaOH solution was slowly added at 70°C. The resulting solution was then aged at the same temperature for 2 hours. In this time period the metal species in the solution were converted into their hydroxide forms. Then, the solution was left to reach room temperature and the clay suspension prepared previously was slowly added on it drop by drop. Thus, the metal to the sepiolite ratio in the final solution was 0.005 mol metal/g sepiolite. The resulting mixture was stirred at 400 rpm for 24 h; throughout this time, the metal hydroxides in the solution were adsorbed on the clay. Then, the solid part of the mixture was separated by filtration, washed repeatedly with distilled water, dried at 60°C overnight and calcined at desired temperatures for 2 hours. At this time period of calcination, the metal hydroxides impregnated on the support material were converted to metal oxide. Unless otherwise stated, the mentioned catalyst in this study was calcined at 500°C.

The AMR value is defined as the molar ratio of the active metal (Fe) to the total content of metals (Fe and

Al) in the metal loadingsolution and can be calculated as follows:

$$AMR(\%) = \frac{mol\ Fe}{mol\ Fe + mol\ Al} \times 100 \quad \dots(1)$$

In experimental studies, catalysts with different AMR values of 0, 2, 4, 6, 8 and 10% were prepared focusing in the CWPO of methyl orange. The catalyst codes were given in Table 1 together with their AMR values.

Characterization methods

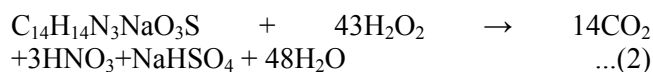
The chemical analyses of the natural sepiolite and SepAlFe8 catalyst were performed by X-ray fluorescence (XRF) using a Rigaku ZSX Primus analyzer. Their X-ray diffraction (XRD) patterns were obtained with a Philips X'Pert Pro device to illuminate the mineralogical structures. The BET specific surface areas and porous properties of the samples were determined from N₂ adsorption experiments using a Quantachrome, Autosorb 1C analyzer. The scanning electron microscopy (SEM) and the energy dispersive X-ray spectroscopy (EDX) analyses were performed with a FEI Quanta 250 FEG scanning electron microscope for the purpose of exploring the surface structures and compositions of natural sepiolite, SepAl and SepAlFe8 samples and the SepAlFe8 sample after experiment.

In order to determine the iron contents of the prepared catalysts, 0.1 g sample was weighed in a baker and 10 mL of distilled water, 10 mL of concentrated HCl and 2 mL of concentrated HNO₃ were added on it. Then the mixture was boiled for about 2 hours and filtered through a filter paper. The iron concentration in the filtrate was determined with a Thermo ICE 3300 model Atomic Absorption Spectrophotometer (AAS) and then the iron percentages in the samples by weight were calculated.

Catalytic experiments

Catalytic experiments were carried out in a heater-jacketed glass reactor at various temperatures (15, 25,

35 and 45°C) under continuous stirring at 200 rpm. For each experiment, the reactor was loaded with desired amount of catalyst and 100 mL of 100 mg L⁻¹ methyl orange solution. The experiments were carried out at different pH values of 3.0, 3.4, 3.7, 4.0 and 4.5 by adjusting the pH with diluted NaOH and HNO₃ solutions. Before starting to feed hydrogen peroxide solution, the mixture was stirred for 15 minutes to achieve adsorption equilibrium between the dye and the catalyst. After this time period, 8.0 mL of freshly prepared 0.15 M H₂O₂ solution was fed into the reactor with the flow rate of 2 mL h⁻¹. The H₂O₂ added was 0.9 times the stoichiometric amount for the complete oxidation of methyl orange (C₁₄H₁₄N₃NaO₃S), according to the following equation:



Samples (2 mL) were taken every 30 mm periodically during 4 hours of reaction time. The liquid part was separated from the medium by centrifugation and the dye concentration in it was determined with a Hach DR 4000 spectrophotometer at a wavelength of 492 nm. Then the methyl orange (MO) elimination rate was calculated using the dye concentrations in the solutions at zero time and any time *t* (min), using the following equation:

$$MO\ elimination\ (\%) = \frac{C_0 - C_t}{C_0} \times 100 \quad \dots(3)$$

Where *C*₀ (mgL⁻¹) is the initial MO concentration and *C*_{*t*} (mgL⁻¹) is the concentration of MO at the time *t* (min). The iron concentrations in the final solutions were also determined by AAS (Thermo ICE 3300) and the iron leaching rates (%) were calculated.

Effects of catalyst amount, metal loading, calcination temperature, pH, H₂O₂ concentration, reaction temperature and time on the MO elimination were investigated. Kinetic data were analysed using the pseudo-first-order and pseudo-second-order kinetic models. The thermodynamic parameters were also determined. The reusability of the SepAlFe8 catalyst was tested through three consecutive CWPO runs.

Results and Discussion

Characterization results

The chemical compositions of natural sepiolite and SepAlFe8 catalyst determined by XRF analyses were given in Table 2. The CaO observed in the raw sepiolite was because of its dolomite (CaMg(CO₃)₂)

Table 1 — The Fe/Al ratios and the AMR values in the metal loading solutions of the catalysts

| Catalyst type | Fe/Al ratio (mol/mol) | AMR (Fe/(Fe+Al)) (mol/mol, %) |
|---------------|-----------------------|-------------------------------|
| SepAl | 0/100 | 0 |
| SepAlFe2 | 2/98 | 2 |
| SepAlFe4 | 4/96 | 4 |
| SepAlFe6 | 6/94 | 6 |
| SepAlFe8 | 8/92 | 8 |
| SepAlFe10 | 10/90 | 10 |

Table 2 — Chemical compositions of the natural sepiolite and SepAlFe8 samples

| Component (%, w/w) | MgO | SiO ₂ | CaO | Fe ₂ O ₃ | Al ₂ O ₃ | LOI |
|-----------------------|-------|------------------|------|--------------------------------|--------------------------------|-------|
| Sepiolite | 30.73 | 48.91 | 2.38 | 0.24 | - | 17.73 |
| SepAlFe8 | 25.26 | 52.80 | - | 4.26 | 8.88 | 8.79 |

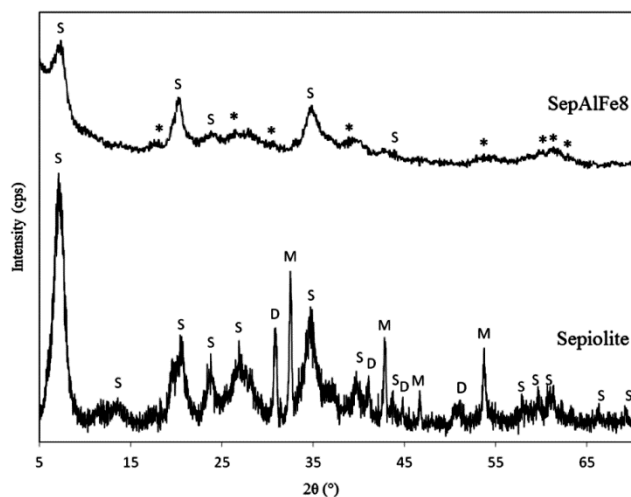


Fig. 1 — XRD patterns of sepiolite and SepAlFe8 catalyst (S: sepiolite, M: magnesite, D: dolomite, *: maghemite or magnetite)

content. The MgO in the mineral composition was mainly caused by sepiolite, and also from magnesite (MgCO_3) and dolomite impurities. In using this information and the XRF elemental results, the sample was determined to consist of approximately 90% wt. sepiolite, 8% wt. dolomite and 2% wt. magnesite. The XRD results of the sepiolite and SepAlFe8 samples were given in Fig. 1. The XRD spectra of natural sepiolite showed the characteristic diffraction reflections of sepiolite clay. It mainly composed of sepiolite and small amounts of magnesite and dolomite. The main reflection was observed in $5^\circ < 2\theta < 9^\circ$ region. This corresponds to the 7.11 (2θ) value from which the interlamellar distance was found to be 12.43 Å. This value was closer to the reported values for several sepiolite samples from Turkey¹¹. The XRD results showed that the catalyst preparation process caused structural changes in the sepiolite sample. After the Al-Fe loading process, the intensity of the 110 reflection has been reduced and its position shifted from 7.11 to 7.46. By this 2θ value, the interlayer distance was calculated as 11.85 Å for SepAlFe8¹⁷. In addition, while sepiolite has an orthorhombic structure, it has turned into a monoclinic structure after metal loading process. The magnesite and dolomite peaks in the XRD of sepiolite sample were not seen in the XRD of SepAlFe8

Table 3 — Textural properties deduced from N₂ adsorption at 77 K for sepiolite and SepAlFe8 samples

| Sample | S_{BET} (m ² g ⁻¹) | V_{micro} (cm ³ g ⁻¹) | V_{total} (cm ³ g ⁻¹) | D_p (Å) |
|-----------|--|---|---|--------------|
| Sepiolite | 182.19 | 0.0054 | 0.2160 | 47.59 |
| SepAlFe8 | 185.90 | 0.0973 | 0.3044 | 65.50 |

(Fig. 1). The CaO component in the sepiolite was completely removed and the amount of MgO component was also decreased during catalyst preparation (Table 2). It can be concluded from these results that magnesite and dolomite ingredients were removed from sepiolite during catalyst preparation process. The increase in the SiO₂:MgO ratio during modification also confirmed this result (Table 2). It can also be seen from the table that the Fe₂O₃ content of sepiolite increased from 0.24% to 4.26% for the SepAlFe8 catalyst. In addition 8.88% Al₂O₃ was determined in this catalyst (Table 2). These were caused by the iron and aluminium species coming from the loading solution. The decrease in the loss on ignition (LOI) value after metal loading was another indicator of the removal of carbonate compounds from the mineral. Namely, sepiolite had magnesite and dolomite impurities and these minerals increased its LOI value. It was reported that dolomite was not decomposed, and sepiolite and dolomite showed a thermally stable behaviour after heat treatment below 700°C. At a temperature of 900°C, dolomite structures broke into CaO by releasing CO₂. Sepiolite was transformed to MgSiO₃ and SiO₂ at the same temperature¹⁸. The new peaks observed in the XRD spectra of SepAlFe8 catalyst indicated the formation of maghemite ($\gamma\text{-Fe}_2\text{O}_3$) or magnetite (Fe₃O₄) on the catalyst. The peaks are very close to the JCPD standards of Fe₂O₃ (JCPDS No. 04-0755) and Fe₃O₄ (JCPDS No. 19-0629). However, the observed reflections are common for maghemite and magnetite, thus, it is difficult to differentiate between the two oxides. The XRD analysis of the catalyst confirmed the occurrence of iron oxidized phase^{19,20}.

The BET specific surface area (S_{BET}) of the natural sepiolite was determined as 182.19 m² g⁻¹ (Table 3). The surface area of the SepAlFe8 catalyst (185.90 m² g⁻¹) slightly increased when compared with the natural clay. In addition, the total pore volume (V_{total}) and especially the micropore volume (V_{micro}) considerably increased.

SEM images magnified at 50000 times for the sepiolite, SepAl and SepAlFe8 catalysts and SepAlFe8

after oxidation experiment were shown in Fig. 2. It could be seen from the SEM image of the natural clay that it had a porous and fibrous morphology [Fig. 2(a)]. There were scattered acicular minerals and mineral aggregates on the surface of it. Among them, the light colored particles were magnesite or dolomite impurities. The results showed that the structure of sepiolite became more porous after the metal loading process [(Figs. 2(b) and (c)]. This result is consistent with the BET analysis (Table 3). SepAlFe8 became much rougher and much more porous. This sample was relatively homogenous. The SEM image of SepAlFe8 after experiment had a similar structure with SepAlFe8 itself [Figs. 2(c) and (d)]. There were some tiny particles on it that might be dye residues or oxidation products.

The EDX results of sepiolite, SepAl, SepAlFe8 and SepAlFe8 after experiment were given in Fig. 3. It could be seen from the figure that Mg ratio on the natural sepiolite was decreased and the Ca component on it was completely removed during catalyst

preparation. These results were consistent with the XRF and XRD results. 4.09% of Al was detected on SepAl, and 3.31% of Al and 2.83% of Fe were observed on SepAlFe8 sample [(Figs. 3(b) and (c)]. It can be seen from the EDX of SepAlFe8 catalyst that Fe/Fe+Al molar ratio on the catalyst (calculated as 29%) was higher than AMR (8%) value. It can also be seen that Fe content of the catalyst after experiment was less than that of SepAlFe8 which showed that small amount of iron was dissolved during the reaction. Furthermore, the appearance of sulfur(S) on the catalyst after experiment at the ratio of 0.43% indicated that methyl orange and/or reaction products (like NaHSO_4) were held on the catalyst.

Effect of catalyst amount

It is well-known that the catalyst loading is an important factor for the industrial utilization in CWPO applications. The effect of catalyst amount on the elimination of methyl orange was investigated using 0.1, 0.3 and 0.5 grams of SepAl catalyst in 100 mL of the dye solution. Experiments were done at pH

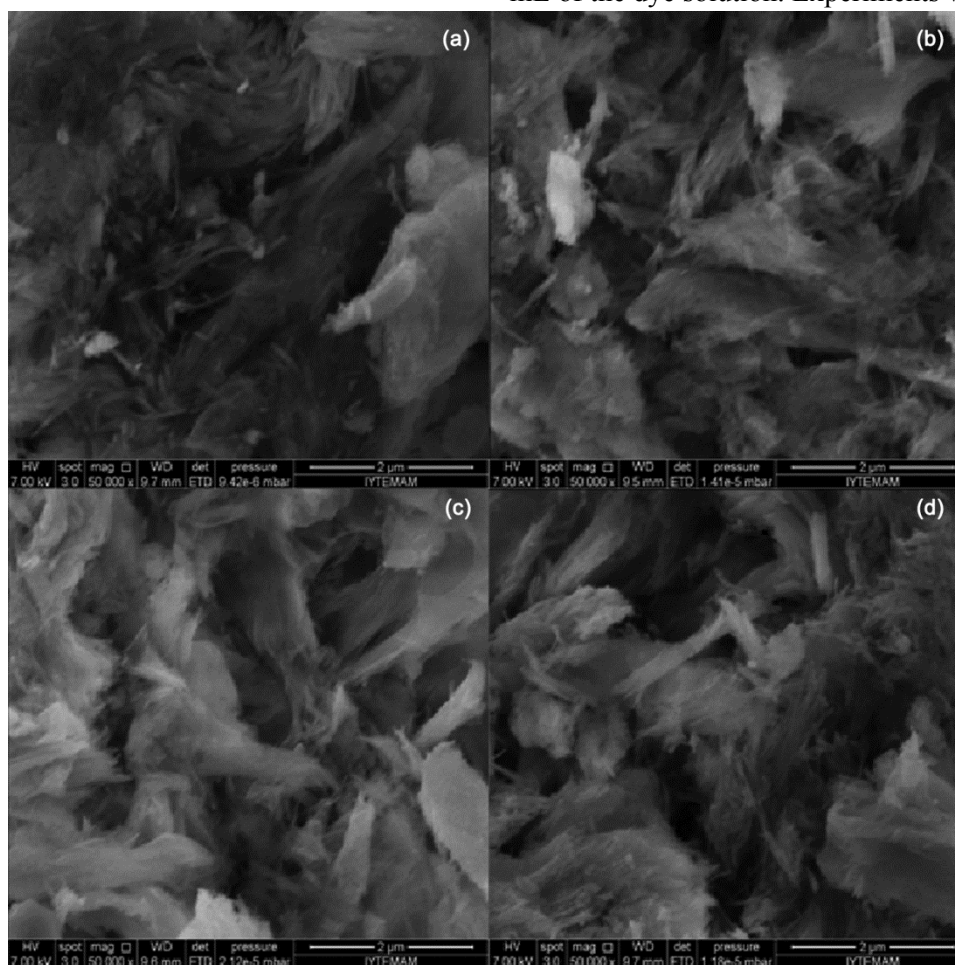


Fig. 2 — SEM images of (a) sepiolite, (b) SepAl, (c) SepAlFe8 and (d) SepAlFe8 after experiment

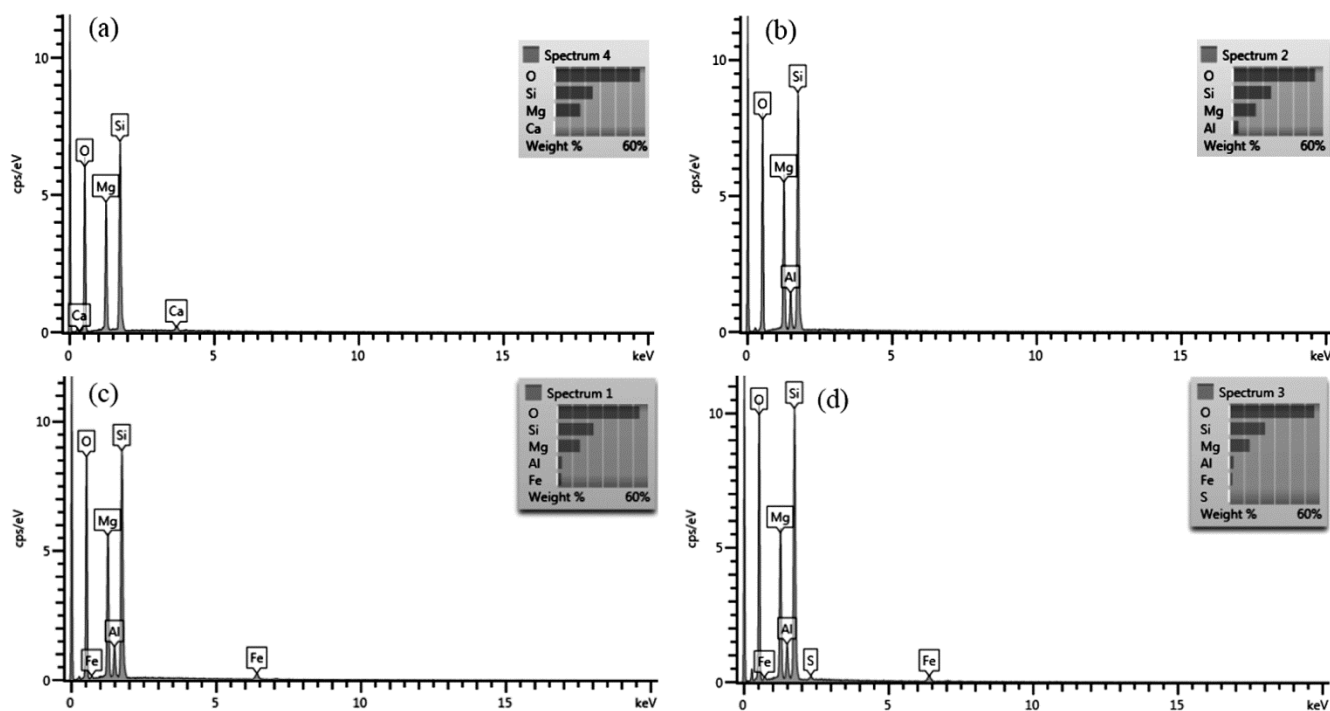


Fig. 3 — EDX of (a) sepiolite, (b) SepAl, (c) SepAlFe8 and (d) SepAlFe8 after experiment

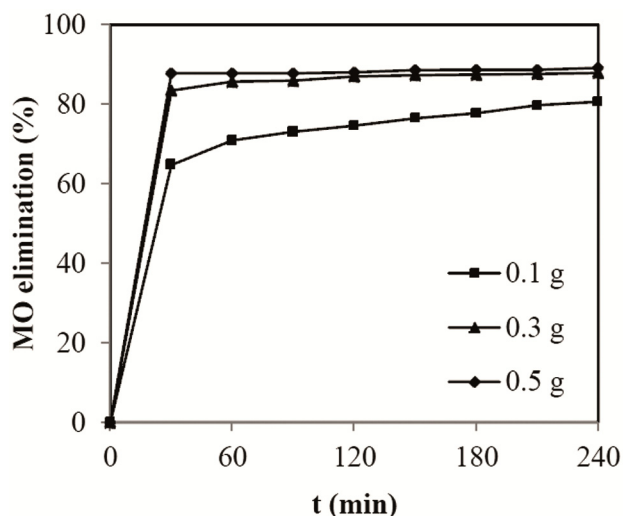


Fig. 4 — Effect of catalyst amount on the MO elimination

3.7 and 25°C with 0.15 M H₂O₂. It could be seen from Fig. 4 that the elimination of methyl orange increased when more amount of catalyst was used since the number of active centers per unit dye amount increased. At the end of 4 hours reaction time, the maximum removal efficiencies of 80.64% for 0.1 g, 87.91% for 0.3 g and 89.15% for 0.5 g catalyst amount were achieved. The heterogeneous Fenton system for the generation of reactive radicals depends on the concentration of hydrogen peroxide and catalyst properties. The methyl orange oxidation

involves firstly the adsorption of the dye molecules on the catalyst surface. In the same way, H₂O₂ is instantaneously adsorbed onto surface of catalyst and broken into powerful oxidizing species reacting with the dye molecules and initiate the oxidative reaction. The high elimination rates at the first 15 min of reaction time implied the adsorption of the dye on the catalyst surface (Fig. 4). It was decided the optimum catalyst amount was 0.1 g due to the catalytic performance, i.e. methyl orange elimination per unit active metal amount, was higher than the others. Therefore, the subsequent experiments were conducted with this amount of catalyst.

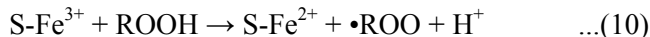
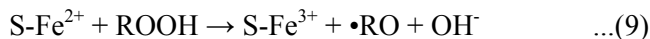
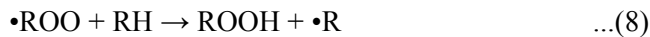
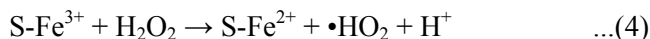
Effect of metal loading

To investigate the effect of metal loading on the dye elimination, oxidation experiments were achieved using catalysts with different active metal ratio ranging from 0% to 10%. The iron contents of the used catalysts determined by AAS after dissolving them in strong acidic medium as explained in “Characterization methods” section were presented in Table 4. As seen from the table that the Fe ratio in the catalysts was increased with increasing active metal ratio as expected. It was also remarkable that the iron contents of the SepAlFe8 and SepAlFe10 catalysts were close to each other, although the value for the SepAlFe10 catalyst was slightly higher. In this series

Table 4 — Iron contents of the catalysts, iron concentrations in the final solutions and iron leaching rates for different catalysts

| Parameter | SepAl | SepAlFe2 | SepAlFe4 | SepAlFe6 | SepAlFe8 | SepAlFe10 |
|--|-------|----------|----------|----------|----------|-----------|
| Fe content (w/w, %) | 0.07 | 0.67 | 1.12 | 1.54 | 2.52 | 2.56 |
| Fe concentration (mg L ⁻¹) | 0.00 | 0.02 | 0.04 | 0.05 | 0.17 | 0.17 |
| Fe leaching rate (%) | 0.00 | 0.30 | 0.36 | 0.32 | 0.67 | 0.66 |

of oxidation experiments, the H₂O₂ concentration fed into the reactor was 0.15 M, the temperature was adjusted to 25°C and the pH value was kept constant at 3.7. The elimination rate was increased with increasing active metal ratio (Fig. 5). At the end of 240 min reaction time, the highest elimination rates of 90.68% and 90.89% were reached when studied with SepAlFe8 and SepAlFe10 catalysts, respectively. In other words, the higher iron rates on the catalyst meant more catalytic sites of iron oxide species for accelerating the decomposition of H₂O₂ to hydroxyl radicals and hence promoted the catalytic oxidation of dye in solution over the prepared catalyst. Hydroxyl radicals are the most oxidizing chemical species after fluorine molecules. By this way, they attack organic pollutants in the solution or the ones adsorbed on the catalyst surface, resulting in oxidation products. The high reactivity of •OH radicals ensures that they will attack a wide range of organic compounds. The mechanism of radical generation in heterogeneous ironoxide containing systems was experimentally verified to occur by surface catalysed decomposition of H₂O₂ as presented below²¹:



where S symbolizes the surface of the catalyst and RH is the organic molecule. By this way, the increasing rate of iron in the catalyst might be increased the elimination yield of the dye by generating more hydroxyl radicals in the solution (Fig. 5).

The iron concentrations in the final solutions determined by the AAS analyses and the leaching rates of iron for the catalysts used were given in Table 4. It can be seen from the table that some part of the iron over the catalysts dissolved in solution during the oxidation. The leaching rate of iron for SepAlFe10 catalyst was determined as 0.66% and the iron

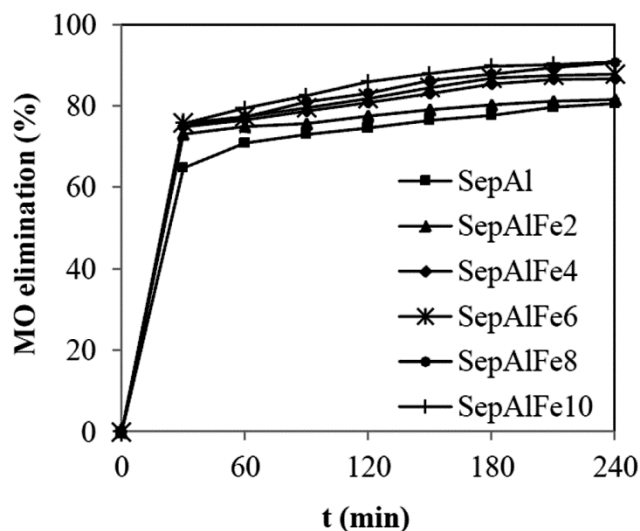


Fig. 5 — Effect of metal loading on the MO elimination

concentration in the final solution was 0.17 mg L⁻¹. These values indicated the methyl orange degradation was accomplished with considerably low leaching of iron.

If the catalytic activity was considered to depend on the amount of active metal in the binary Fe+Al mixture, while the active metal ratio increased the catalytic performance per active center decreased significantly (Fig. 6). High active metal ratio caused to deteriorate excessively the critical physicochemical properties, such as textural properties and to form external aggregates²². For this reason, the best results per active center were obtained for the 2% active metal ratio in which the absorbed iron on the sepiolite formed more active phase.

Since the elimination rates for SepAlFe8 and SepAlFe10 were almost the same as seen in Fig. 5 and the iron content of the SepAlFe8 was lesser (Table 4), this catalyst was selected as the best one and used in subsequent experiments.

Effect of calcination temperature

The effect of calcination temperature was examined by using SepAlFe8 catalysts calcined at different temperatures in the range of 400-700°C. The tests were achieved at pH 3.7 and 25°C with 0.1 g of catalyst and 0.15 M H₂O₂. The elimination of methyl orange increased with increasing calcination temperature, as seen in Fig. 7. The elimination rates

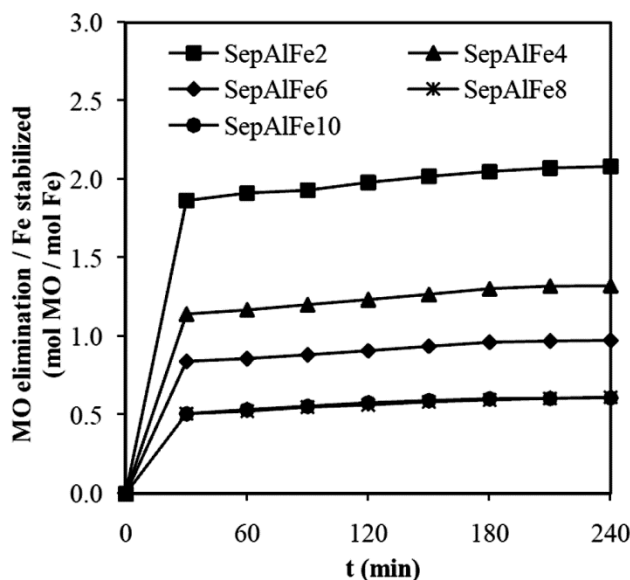


Fig. 6 — Catalytic performance of catalysts referred to the net amount of active metal stabilized

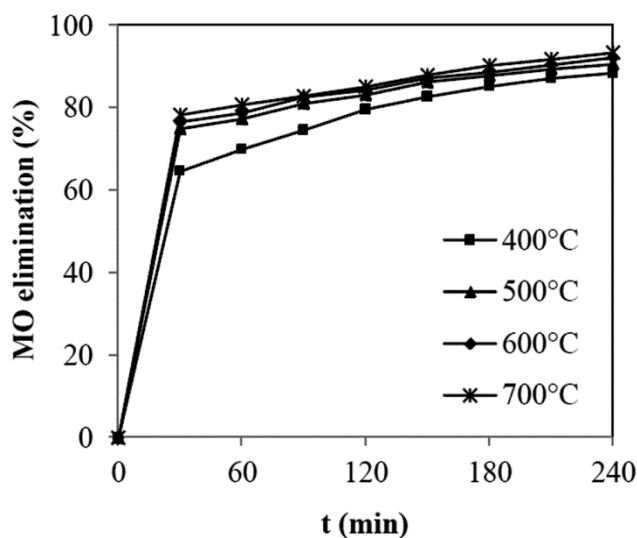


Fig. 7 — Effect of calcination temperature on the MO elimination
 were very close to others for the catalysts calcined at 500°C, 600°C and 700°C. Moreover, the weight losses of the catalyst during the calcination at 400°C, 500°C, 600°C and 700°C temperatures were determined as 8.83%, 10.61%, 14.72% and 18.73%, respectively. According to these results, the weight loss values of 600°C and 700°C were significantly higher than that of 500°C. Thus, one can estimate that a higher calcination temperature means the necessity of more amounts of support material and metals, in addition more energy consumption to prepare a certain amount of catalyst. By considering these results, the most appropriate calcination temperature was decided as 500°C to cause lower energy

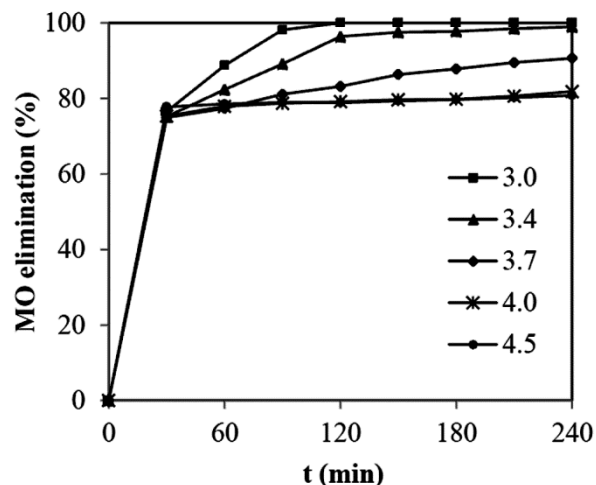


Fig. 8 — Effect of pH on the MO elimination

Table 5 — Iron concentrations in the final solutions and iron leaching rates for different pH values

| pH | 3.0 | 3.4 | 3.7 | 4.0 | 4.5 |
|---|------|------|------|------|------|
| Fe concentration (mg L^{-1}) | 1.79 | 0.81 | 0.17 | 0.03 | 0.02 |
| Fe leaching rate (%) | 7.10 | 3.21 | 0.67 | 0.12 | 0.08 |

consumption and lesser weight loss during the calcination while achieving a high enough elimination.

Effect of pH

The hydroxyl radical and dye properties are both effective on the decolorization of dye solution, and generally decolorization rates of dyes by oxidation process decrease with increasing pH since H_2O_2 is converted to its less reactive conjugate base in alkaline solutions. The oxidation of methyl orange over the SepAlFe8 catalyst was studied under the different pH values of 3.0, 3.4, 3.7, 4.0 and 4.5 to investigate the effect of pH value of the reaction medium. The other parameters were 0.1 g for catalyst amount, 500°C for calcination temperature, 0.15 M for H_2O_2 concentration and 25°C for reaction temperature. The results obtained from the pH study were depicted in Fig. 8. It clearly seen that the elimination of MO was increased when the pH value decreased. Even, the elimination value reached 100% at the end of 120 min when studied at pH 3.0. But as a negative aspect of pH, the iron leaching rates increased at lower pH values (Table 5). This meant the catalyst was not stable at lower pH values and would decompose into fewer cycles. Thus, the optimum pH value was selected as 3.7 to provide dye elimination highly enough and in the meantime to avoid a high iron leaching. In the literature, the optimum pH value for Al-Fe loaded materials was reported in the range of 3.5-4^{22,23}. It is also stated that

this pH range correspondsto the highest stability region of the soluble $\text{Fe}(\text{OH})^{2+}$ complex²³.

Effect of H_2O_2 concentration

To investigate the effect of H_2O_2 concentration on the MO removal, experiments were carried out with SepAlFe8 catalyst calcined at 500°C , by feeding H_2O_2 solutions at different concentrations ranging from 0.05 M to 0.20 M while the other experimental parameters kept constant at 0.1 g for catalyst amount, 3.7 for pH and 25°C for temperature (Fig. 9). Although the increase was not high, it was seen that the elimination of MO increased with increasing H_2O_2 concentration. In fact, almost the same MO elimination values were reached when studied with the concentrations of 0.15 M and 0.20 M. Therefore, the optimum H_2O_2 concentration was selected as 0.15 M.

In addition, experiments wererepeatedby using only H_2O_2 or only catalyst alone, to test their single effects on the dye removal (Fig. 10). When both of the catalyst and H_2O_2 were used together (the standard

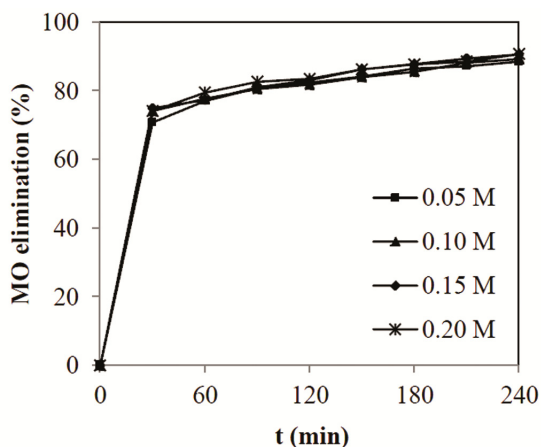


Fig. 9 — Effect of H_2O_2 concentration on the MO elimination

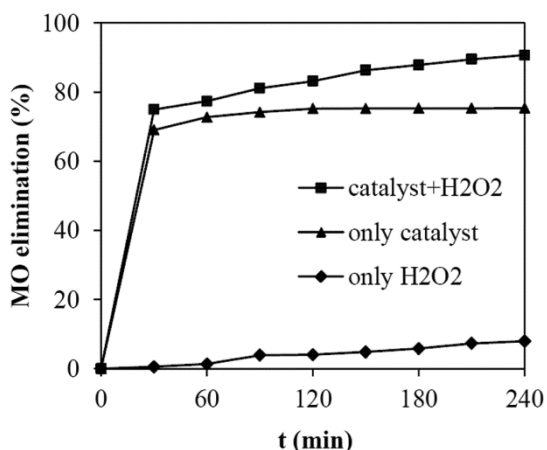


Fig. 10 — Effect of single and binary usage of catalyst and H_2O_2 on the MO elimination

test), the elimination rateof 90.68% was achieved at the end of 4 h. It was observed at the experiment without catalyst that the removal efficiency was 7.90%. The oxidation ability of H_2O_2 was very limited under these mild conditions. This removal rate was much lower than that of the standard test. The iron oxide phase on the catalyst was beneficial to act with H_2O_2 , thus generate more $\bullet\text{OH}$ radicals to degrade MO molecule in the standard test. In addition, 75.37% of dye removal was achieved when the catalyst used alone. This showed that the catalyst was removed the dye by the way of adsorption. Similar adsorptive removals were reported in some previous studies^{2,24,25}.

Effect of reaction temperature and kinetics

The oxidation experiments were repeated at four different temperatures of 15°C , 25°C , 35°C and 45°C in order to assess the effect of the temperature on the elimination rate of methyl orange dye. The elimination rates at the end of 4 hoursreaction time increased from 87.85% to 93.54% with increasing temperaturefrom 15°C to 45°C (Fig. 11). As expected, the increase in temperature accelerated the reaction rate between H_2O_2 and the catalyst to form hydroxyl radicals ($\bullet\text{OH}$) leading to high decolorization rates²⁴. Conversely, the elimination rates observed after first 30 min decreased with increasing temperature. This might be caused by the adsorptive removal decreased with increasing temperature. Furthermore, the Fe concentrations in the final solutions and the leaching rates determined for the experiments temperature effect investigated were presented in Table 6. As seen in the table, the leaching rates increased with increasing temperature. On the other hand, the low values of iron concentration ($<0.3 \text{ mgL}^{-1}$) pointed out

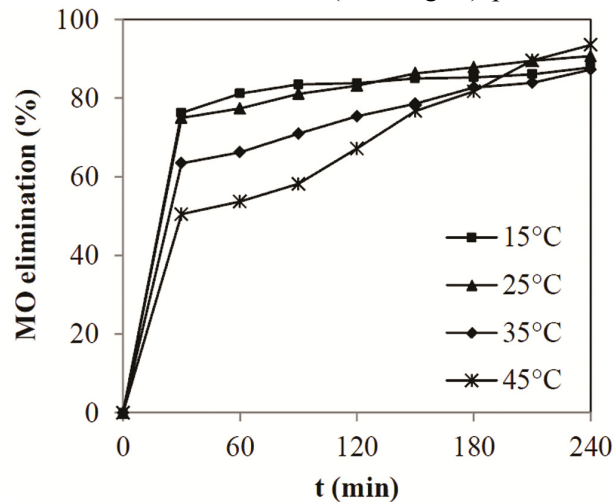


Fig. 11 — Effect of temperature on the MO elimination

the active phase strongly fixed to the catalyst structure and thus, the catalyst was highly stable under mildly acidic conditions of oxidizing medium.

According to previous studies relating to the heterogeneous Fenton oxidation, the kinetic degradation of organic compounds under this system fits pseudo-first-order and pseudo-second-order kinetic models^{16,26}. Therefore, the catalytic wet peroxide oxidation of methyl orange dye over SepAlFe8 catalyst was modelled by using these two kinetic models. The linearized kinetic rate expression for pseudo-first-order kinetic model can be expressed as:

$$\ln C_t = \ln C_0 - k_1 t \quad \dots(11)$$

Where C_0 and C_t (mol L⁻¹) are the concentrations of methyl orange initially and at any time t (min), respectively, and k_1 (min⁻¹) represents the pseudo-first-order rate constant. The pseudo-second-order kinetic model is simply given as:

$$\frac{1}{C_t} = \frac{1}{C_0} + k_2 t \quad \dots(12)$$

Where k_2 is the pseudo-second-order rate constant (mol L⁻¹ min⁻¹). Values of k_1 and k_2 calculated respectively from the slopes of $\ln C_t$ versus t and $1/C_t$ versus t plots at various temperatures (plots not shown) were given in Table 7. As expected, k_1 values increased with increasing temperature, but the k_2 values fluctuated. In addition, determination coefficients (R^2) given in the table were found to be higher for pseudo-first-order kinetic model, therefore, kinetic data was found to be better represented by pseudo-first-order kinetic model. The increase in the rate constant (k_1) with temperature has proven that higher temperatures lead to an increase in the production of •OH and thus to an increase in MO conversion.

Table 6 — Iron concentrations in the final solutions and iron leaching rates for different temperatures

| T (°C) | 15°C | 25°C | 35°C | 45°C |
|--|------|------|------|------|
| Fe concentration (mg L ⁻¹) | 0.17 | 0.17 | 0.22 | 0.28 |
| Fe leaching rate (%) | 0.67 | 0.67 | 0.87 | 1.11 |

Table 7 — Kinetic parameters for the degradation of methyl orange

| T (°C) | Pseudo-first-order kinetic model | | Pseudo-second-order kinetic model | |
|--------|----------------------------------|-------|--|-------|
| | k_1 (min ⁻¹) | R^2 | k_2 (mol L ⁻¹ min ⁻¹) | R^2 |
| 15 | 0.0027 | 0.961 | 59.57 | 0.962 |
| 25 | 0.0049 | 0.996 | 104.40 | 0.985 |
| 35 | 0.0051 | 0.991 | 70.22 | 0.936 |
| 45 | 0.0097 | 0.931 | 156.21 | 0.727 |

Thermodynamics of the catalytic reaction

Using the pseudo-first-order rate constants (k_1), the apparent activation energy (E_a) and the Arrhenius factor (A) were determined by the Arrhenius equation given in the following equation:

$$k_1 = A \cdot \exp^{-E_a/RT} \quad \dots(13)$$

The values of E_a (kJ mol⁻¹) and A (min⁻¹) were obtained from the slope and intercept of $\ln k_1$ versus $1/T$ plot (Fig. 12). It was found that there was good linear relation between $\ln k_1$ and $1/T$ with $R^2 = 0.9154$. The values of E_a and A were found to be 29.48 kJ mol⁻¹ and 621.29 min⁻¹ for pseudo-first-order kinetic model, respectively. Schlichter *et al.* were reported the oxidation of MO fitted the first-order kinetic model for copper heterogeneous catalysts prepared with MCM-41 and SBA-16 supports. They were also reported the E_a values were 42 kJ mol⁻¹ and 28 kJ mol⁻¹ for Cu/SBA-16-NH₂ and Cu/MCM-41-24 catalysts, respectively²⁷. In another study²⁸, the E_a value for the removal of MO by Si/Al@Fe/MWCNT in the presence of H₂O₂ was reported as 44.1 kJ mol⁻¹. In addition, the activation energy of Fenton reaction was reported to be usually in 20.7–56.1 kJ mol⁻¹ under different heterogeneous catalysts²⁹. Thus, the activation energy required for the oxidation of MO by SepAlFe8 concluded to be low when compared the studies given above.

The degradation process was reported to be surface-controlled when E_a was higher than 29 kJ mol⁻¹, and diffusion-controlled when E_a ranges from 8 to 21 kJ mol⁻¹^{28,30}. The calculated E_a value for MO degradation over SepAlFe8 catalyst showed that it was a surface-controlled process. According to the findings above the recitation mechanism could be

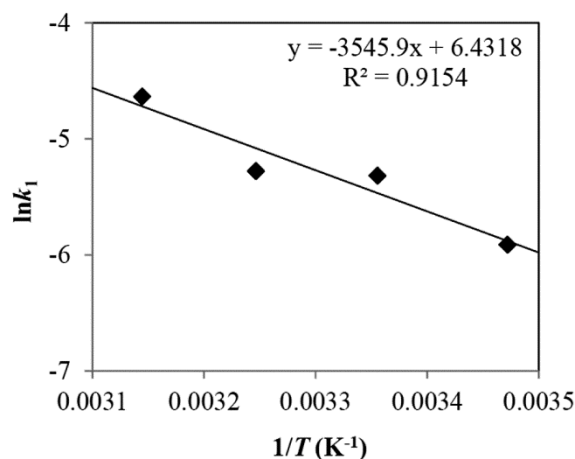


Fig. 12 — Arrhenius plot for the pseudo-first-order rate constants of the oxidation of methyl orange over SepAlFe8 catalyst

explained as: first the hydroperoxyl ($\bullet\text{HO}_2$) and hydroxylradicals ($\bullet\text{OH}$) produced via Fe^{3+} react with the adsorbed H_2O_2 (Eqs. 4 and 5). Second, the MO molecules absorbed on SepAlFe8 are attacked by the $\bullet\text{OH}$ absorbed on the surface of the catalyst, and the reaction intermediates are obtained. Then, the intermediates completely decompose to H_2O and CO_2 . Changes in enthalpy (ΔH) and entropy (ΔS) describe the reaction either through endothermic or exothermic reaction pathways. In this study, the enthalpy and entropy changes were calculated using the following Eyring equation:

$$\ln \frac{k_1}{T} = \ln \frac{k_b}{h} + \frac{\Delta S}{R} - \frac{\Delta H}{RT} \quad \dots(14)$$

Where k_1 is the reaction rate constant, k_b is the Boltzmann's constant ($1.38 \times 10^{-23} \text{ J K}^{-1}$) and h is the Planck's constant ($6.63 \times 10^{-34} \text{ J s}$), R is the universal gas constant ($8.314 \text{ J mol}^{-1} \text{ K}^{-1}$) and T is the absolute temperature (K). The values of ΔH and ΔS were calculated from the slope and intercept of $\ln(k_1/T)$ versus $1/T$ (plot not shown). A positive value of $26.99 \text{ kJ mol}^{-1}$ for ΔH indicated the reaction experienced the endothermic pathway whereby the heat energy was absorbed to bring the reactants to transition state towards the products. A negative value of $-233.86 \text{ J mol}^{-1} \text{ K}^{-1}$ for ΔS showed that the system was less disordered, namely most of the energy inputs were channeled into the reaction rather than dispersing out. In addition, the Gibbs free energy (ΔG) at 25°C was calculated using Gibbs Helmholtz equation (Eq. 15). A positive value of $96.72 \text{ kJ mol}^{-1}$ for ΔG showed the reaction was nonspontaneous.

$$(\Delta G = \Delta H - T\Delta S) \quad \dots(15)$$

Reusability studies of the prepared catalyst

Recycling of the catalysts is frequently problematic because of their instability and leaching characters. In order to investigate the stability degree of the prepared catalyst (SepAlFe8) upon degradation of MO dye solution (pH 3.7), the catalyst separated from solution by filtration at the end of the experiment and used again after re-calcination at 500°C for 2 hours. This process was carried out for 3 cycles at 25°C and the results were depicted in Fig. 13. Furthermore, the iron concentrations in the final solutions of the oxidation experiments were determined by AAS, and then the iron leaching rates were calculated and given in Table 8. As seen in Fig. 13, MO elimination rates slightly decreased from 90.68% for the first cycle to 88.42% and 86.18% for the second and third cycles, respectively. The iron content of the catalyst

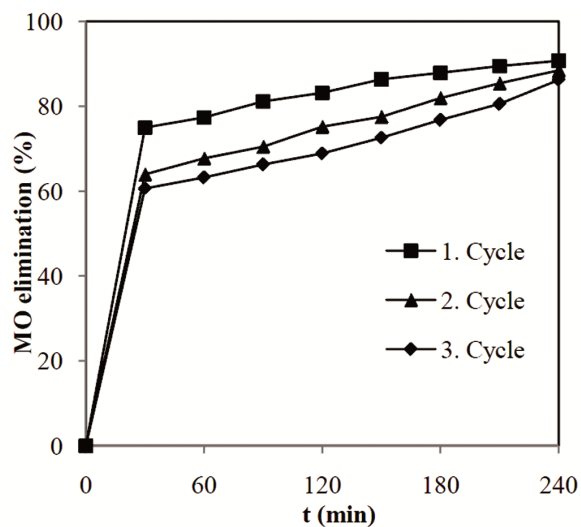


Fig. 13 — Effect of the reuse of catalyst on the MO elimination

Table 8 — Iron concentrations in the final solutions and iron leaching rates for three cycles

| Cycles | 1 st cycle | 2 nd cycle | 3 rd cycle |
|---|-----------------------|-----------------------|-----------------------|
| Fe concentration (mg L^{-1}) | 0.17 | 0.18 | 0.23 |
| Fe leaching rate (%) | 0.67 | 0.71 | 0.91 |

decreased a bit in every cycle because of the dissolution of the metal in the acidic medium (Table 8). This may be responsible from the decrease in MO elimination; but, it should also be kept in mind that after each cycle some contaminants may remain on the catalyst and might affect the elimination rate.

Conclusion

In the present study, Al-Fe loaded sepiolite catalysts were synthesized and tested in the CWPO of the methyl orange azo dye. The natural sepiolite and the catalysts were characterized by XRD, XRF, BET, SEM and EDX techniques. The presence of the iron oxide phase on the catalyst was proved by the XRD analysis. The iron content of the catalysts was determined to increase with increasing active metal ratio. The BET specific surface area of the catalyst was slightly higher than that of sepiolite. The catalyst was determined to have more porous and homogenous structure. The effects of various operational parameters such as catalyst amount, metal loading, calcination temperature, pH, H_2O_2 concentration, reaction temperature and time were examined. The SepAlFe8 calcined at 500°C was chosen as the best catalyst in terms of activity and stability. In addition, catalyst amount of 0.1 g, pH of 3.7, H_2O_2 concentration of 0.15 M and temperature of 25°C were selected as optimum conditions. 90.68% of

methyl orange elimination was attained after 4 h of oxidation reaction under these optimum conditions. Moreover, the low concentration of iron in the final solution (0.17 mg L^{-1}) was indicated the catalyst to have a strong structure. Kinetic studies showed the oxidation reaction of MO over SepAlFe8 catalyst obeyed the pseudo-first-order kinetic expression. The activation energy was found to be $29.48 \text{ kJ mol}^{-1}$. In addition, the reaction was determined as endothermic and nonspontaneous. The thermodynamic parameters were determined as $26.99 \text{ kJ mol}^{-1}$ for ΔH , $-233.86 \text{ J mol}^{-1} \text{ K}^{-1}$ for ΔS and $96.72 \text{ kJ mol}^{-1}$ for ΔG . The reusability of the catalyst was experimented through threeconsecutive cycles under the optimum conditions and it afforded highly decomposition of MO dye over 85% within the third CWPO run. Consequently, the Al-Fe loaded sepiolite could potentially be used as a proficient catalyst through CWPO processes.

References

- 1 Samoila P, Cojocaru C, Sacarescu L, Dorneanu P P, Domocos A & Rotaru A, *Appl Catal B-Environ*, 202 (2017) 21.
- 2 Drasinac N, Erjavec B, Drazic G & Pintar A, *Catal Today*, 280 (2017) 155.
- 3 Han J, Zeng H Y, Xu S, Chen C R & Liu X J, *Appl Catal A Gen*, 527 (2016) 72.
- 4 Pinho M T, Silva A M T, Fathy N A, Attia A A, Gomes H T & Faria J L, *J Environ Chem Eng*, 3 (2015) 1243.
- 5 Ribeiro R S, Silva A M T, Figueiredo J L, Faria J L & Gomes H T, *Appl Catal B Environ*, 187 (2016) 428.
- 6 Zazo J A, Bedia J, Fierro C M, Pliego G, Casas J A & Rodriguez J J, *Catal Today*, 187 (2012) 115.
- 7 Brauner K & Preisinger A, *Tscher Mineral Petr Mitt*, 6 (1956) 120.
- 8 Alkan M, Tekin G & Namli H, *Micropor Mesopor Mat*, 84 (2005) 75.
- 9 Suarez M & Garcia-Romero E, *Appl Clay Sci*, 67 (2012) 72.
- 10 Lazarevic S, Jankovic-Castvan I, Jovanovic D, Milonjic S, Janackovic D & Petrovic R, *Appl Clay Sci*, 37 (2007) 47.
- 11 Suarez M, Garcia-Rivas J, Garcia-Romero E & Jara N, *Appl Clay Sci*, 131 (2016) 124.
- 12 Işik I, Uz V, Austin G S & Işik C E, *Appl Clay Sci*, 49 (2010) 29.
- 13 Jin L, Zeng H Y, Xu S, Chen C R, Duan H Z, Du J Z, Hu G & Sun Y X, *Chinese J Catal*, 39 (2018) 1832.
- 14 Thao N T & Nhu N T, *J Sci Adv Mater Devices*, 3 (2018) 289.
- 15 Zhang J, Yan Z, Fu L, Zhang Y, Yang H, Ouyang J & Chen D, *Appl Clay Sci*, 166 (2018) 166.
- 16 Zhou F, Yan C, Liang T, Sun Q & Wang H, *Chem Eng Sci*, 183 (2018) 231.
- 17 Eren E, Gumus H & Ozbay N, *Desalination*, 262 (2010) 43.
- 18 Meşe E, Figen A K, Filiz B C & Pişkin S, *Appl Clay Sci*, 153 (2018) 95.
- 19 Orolinova Z & Mockovciakova A, *Mater Chem Phys*, 114 (2009) 956.
- 20 Lu Z, Hao Z, Wang J & Chen L, *J Ind Eng Chem*, 34 (2016) 374.
- 21 Khankhasaeva S T, Dashinamzhilova E T & Dambueva D V, *Appl Clay Sci*, 146 (2017) 92.
- 22 Galeano L A, Gil A & Vicente M A, *Appl Catal B-Environ*, 100 (2010) 271.
- 23 Barrault J, Abdellaoui M, Bouchoule C, Majeste A, Tatibouet J M, Louloudi A, Papayannakos N & Gangas N H, *Appl Catal B-Environ*, 27(2000) 225.
- 24 Fathy N A, El-Khouly S M, Hassan N A & Awad R M S, *J Water Process Eng*, 16 (2017) 21.
- 25 Qin H, Xiao R & Chen J, *Sci Total Environ*, 626 (2018) 1414.
- 26 Subbaramaiah V, Srivastava V C & Mal I D, *J Hazard Mater*, 248 (2013) 355.
- 27 Schlichter S, Sapag K, Dennehy M & Alvarez M, *J Environ Chem Eng*, 5(2017) 5207.
- 28 Arshadi M, Abdolmaleki M K, Mousavinia F, Khalafi-Nezhad A, Firouzabadi H & Gil A, *Chem Eng Res Des*, 112 (2016) 113.
- 29 Liu J, Cui J, Zhao T, Fan S, Zhang C, Hu Q & Hou X, *Colloid Surface A*, 565 (2019) 59.
- 30 Ren B, Xu Y, Zhang C, Zhang L, Zhao J & Liu Z, *J Taiwan Inst Chem E*, 97 (2019) 170.